

# Environmental Science Nano

Accepted Manuscript

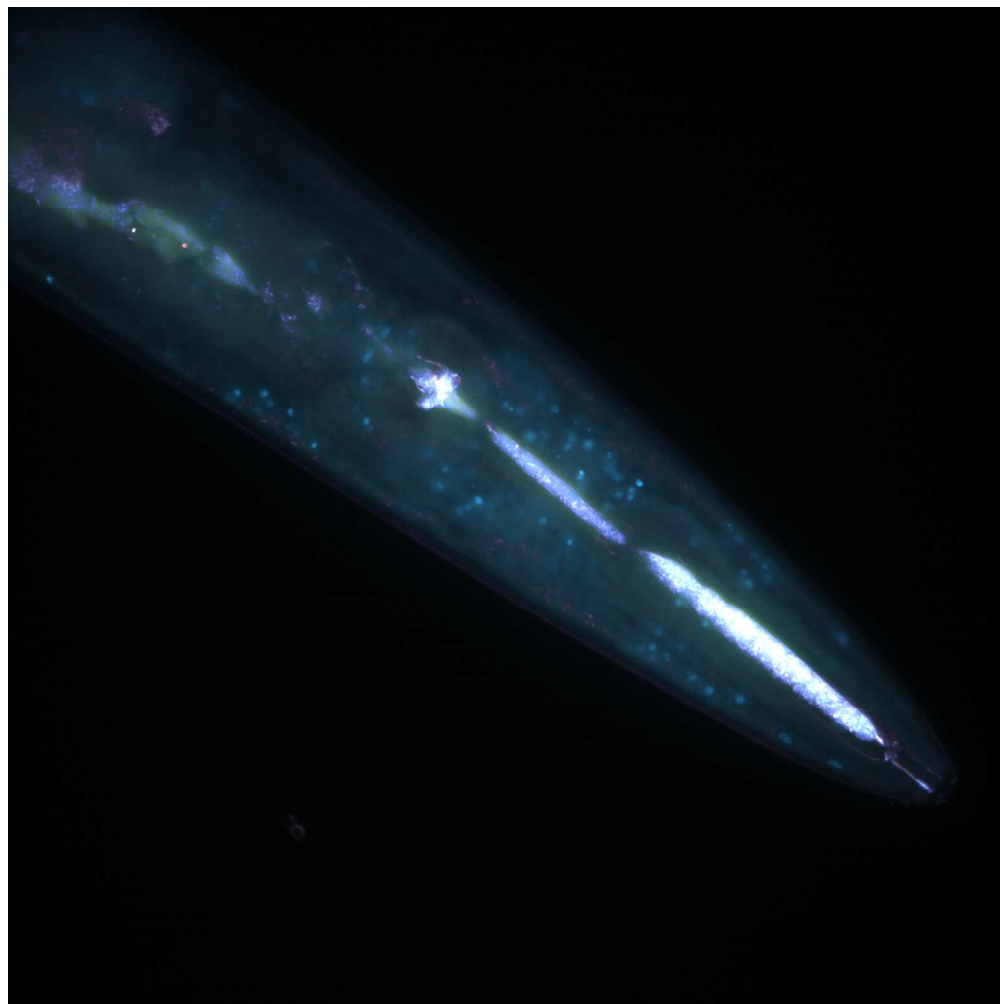


This is an *Accepted Manuscript*, which has been through the Royal Society of Chemistry peer review process and has been accepted for publication.

*Accepted Manuscripts* are published online shortly after acceptance, before technical editing, formatting and proof reading. Using this free service, authors can make their results available to the community, in citable form, before we publish the edited article. We will replace this *Accepted Manuscript* with the edited and formatted *Advance Article* as soon as it is available.

You can find more information about *Accepted Manuscripts* in the [Information for Authors](#).

Please note that technical editing may introduce minor changes to the text and/or graphics, which may alter content. The journal's standard [Terms & Conditions](#) and the [Ethical guidelines](#) still apply. In no event shall the Royal Society of Chemistry be held responsible for any errors or omissions in this *Accepted Manuscript* or any consequences arising from the use of any information it contains.



Halloysite nanotubes in *C. elegans* foregut (merged enhanced dark field and fluorescence image)  
541x541mm (96 x 96 DPI)

## Toxicity of halloysite clay nanotubes *in vivo*: a *Caenorhabditis elegans* study

Gölnur I. Fakhrullina,<sup>a</sup> Farida S. Akhatova,<sup>a</sup> Yuri M. Lvov<sup>b</sup> and Rawil F. Fakhrullin<sup>a\*</sup>

<sup>a</sup>Bionanotechnology Lab, Department of Microbiology, Institute of Fundamental Medicine and Biology, Kazan Federal University, Kremlyuramı 18, Kazan, Republic of Tatarstan, Russian Federation, 420008

<sup>b</sup>Institute for Micromanufacturing, Louisiana Tech University, 911 Hergot Ave., Ruston, LA 71272, USA

### ABSTRACT

Here we investigated the toxicity of halloysite clay nanotubes *in vivo* employing the nematode *Caenorhabditis elegans* as a model organism. Using enhanced dark-field microscopy and physiological tests, we found that halloysite is localised exclusively in the alimentary system and does not induce severe toxic effects on nematodes.

### NANO IMPACT

Halloysite is a nanomaterial which is already used in tens of thousand tons in ceramic and polymeric composite industry. These clay tubes are excavated from the mines as a stone mineral and processed by milling to fine powder of 50 nm diameter and 1.5  $\mu\text{m}$  length tubes. This treatment converts environmentally safe minerals to potentially dangerous nano-dispersed material. The halloysite nanotubes were found to be not toxic for isolated cell cultures, but no *in vivo* studies were performed for whole organisms. We analysed the nanosafety of halloysite for soil nematodes (*Caenorhabditis elegans*), one of the first organisms which may encounter these nanotubes in the polluted soil. Halloysite nanotubes were found safe for *C. elegans* at the concentration up to 1 mg/mL which is of about 1000 times higher than the possible soil contamination concentrations.

Halloysite nanotubes (HNTs) are regarded as one of the most promising natural nanoscale materials. This clay nanomaterial has recently attracted an attention due to its extraordinary chemical and physical properties, cheap production and availability in thousand tons. Halloysite is a natural clay material, chemically identical to kaolin, having outer diameter of 40–70 nm, inner diameter of 10–20 nm and length of 500–1500 nm.<sup>1</sup> Halloysite tubes are a rolled kaolin aluminosilicate sheets, where the internal side composed of  $\text{Al}_2\text{O}_3$ , while the external is  $\text{SiO}_2$ , which allows for the selective chemical modification of these outer / inner surfaces.<sup>2</sup> Halloysite is excavated from the mines as white rocks containing 95–99 wt. % of nanotubes and remaining are kaolin, quartz and iron oxide admixtures. Halloysite is well mixable with many polymers: from synthetic polyethylene, polypropylene, epoxy resins and polyamides to natural polysaccharides and gelatin. Typically, doping polymers with 4–5 wt. % halloysite increases the composite strength and adhesivity on 40–50 % and effectively improves its flame-retardance.<sup>1</sup> The large surface area and oppositely-charged inner and outer layers facilitate loading of negatively charged biomacromolecules into a positive tubes' lumen (e.g., DNA encapsulation). As a result, halloysite nanotubes have been found applicable for fabrication of novel biomedical materials with controlled release, i.e. drug<sup>3–6</sup> or enzyme<sup>7</sup> carriers, gene delivery vehicles,<sup>8</sup> antibacterial coatings,<sup>9</sup> nanostructured coatings for improved adhesion of human cells,<sup>10,11</sup> cell surface engineering,<sup>12</sup> and scaffolds for tissue engineering.<sup>13</sup> Equally important, pristine and functionalized halloysite nanotubes were utilised in numerous industrial applications as inorganic micelles to capture hydrocarbon and aromatic oils,<sup>14</sup> corrosion inhibitors,<sup>15,16</sup> organic films stabilizers,<sup>17</sup> filtration membranes<sup>18</sup> and catalyst supports,<sup>19,20</sup> among many others.

Annually, approximately 30,000 tons of halloysite clay minerals are excavated worldwide and processed to dispersed nanotubes.<sup>1</sup> These nanotubes are added into ceramic and polymer composites, besides potential doping them into auto tire rubber which may bust halloysite pollution is under consideration.<sup>21</sup> Rapidly expanding use of halloysite nanotubes in porcelain and polymer composite industry<sup>22</sup> suggests a high probability of undesired release of HNTs into environment, bringing them into the direct contact with organisms in their natural habitats, which may potentially cause unwanted damage to cells, tissues and organs. Therefore, the elucidation of the toxicity of halloysite nanotubes towards living organisms is crucially important.

Several recent reports demonstrate the investigation of halloysite nanotoxicity *in vitro*, employing human cell cultures and microbial cells. The toxicity and cellular uptake of halloysite nanotubes was investigated using human breast cancer cells and human epithelial adenocarcinoma cells.<sup>23</sup> The cells were cultivated in media supplemented with increasing halloysite concentrations, consequently the distribution of nanotubes in cytoplasm was mapped with confocal microscopy, while the viability of the cells was assessed using enzymatic activity tests. The results suggest that the viability of the halloysite-treated cells (up to 0.075 mg/mL) was preserved (up to 70% of viable cells), however, at higher concentrations of HNTs (from 1 mg/mL), cell death was induced in both types of cells. Relatively low toxicity of chitosan-based scaffolds for tissue engineering was demonstrated by monitoring the growth of fibroblasts on nanocomposites.<sup>13</sup> No significant effects of fibroblasts attachment and development on chitosan-doped scaffold were observed. In proteomic analysis, exposure-specific changes in expression observed among 4081 proteins have shown pro-inflammatory effects at halloysite exposures as low as 1 mg mL<sup>-1</sup> and significant changes in protein expression at very high concentration of 100 mg mL<sup>-1</sup>. Based on these findings, halloysite clay nanotubes appear unlikely to have toxic effects at moderate levels of exposure. Bioinformatic analysis of differentially expressed protein profiles suggest that halloysite stimulates processes related to cell growth and proliferation, subtle responses to cell infection, irritation and injury, enhanced antioxidant capability, all characteristic of an overall adaptive response to exposure.<sup>24</sup> Moreover, halloysite-doped polymer dental scaffolds stimulated the growth of dental pulp fibroblast cells.<sup>25</sup>

The extent of toxicity of HNTs on microbial communities is not completely understood yet. According to Zhang et al., pristine HTNs exhibits little toxicity towards *Escherichia coli* bacteria<sup>26</sup>, however, another report suggests that the pristine halloysite exhibited the highest toxicity to *E. coli*.<sup>27</sup> The toxic effects of pristine HNTs are likely to be caused by the direct contact of nanotubes with cell walls and reactive oxygen generation.<sup>27</sup> On the other hand, HTNs were shown to be non-toxic towards yeast cells.<sup>12</sup> These ambiguous results stimulate the further investigation of halloysite toxicity. Importantly, the *in vivo* investigations are required,<sup>28</sup> since the toxic effects of nanomaterials on isolated cell culture may not be directly extrapolated onto the whole organisms.

Here we report for the first time the *in vivo* toxicity testing of halloysite nanotubes employing a free-living nematodes *Caenorhabditis elegans* as a model organism. These nematodes have been extensively used in a number of biological studies, including toxicity assays. *C. elegans* nematode is an extremely important tool in molecular biology because its fully sequenced genome is closely homologous to the human genome, its relatively short life span takes only three weeks and its tiny transparent ~1 mm-long body is built up from about 960 cells.<sup>29,30</sup> Previously, *C. elegans* nematodes were found to be a versatile animal model for nanotoxicity assays to evaluate the toxicity of carbon nanotubes,<sup>31,32</sup> gold,<sup>33</sup> silica<sup>34</sup> and metallofullerene nanoparticles,<sup>35</sup> and graphite nanoplatelets.<sup>36</sup> Aiming at the toxicity tests of halloysite nanotubes, we have chosen *C. elegans* wild type (Bristol N2) microworms for the following reasons: 1) *C. elegans* naturally populate soils, therefore they are likely to encounter the product-released HNTs; 2) they are optically transparent and small-sized animals, which allows to directly

visualise HNTs distribution using enhanced dark-field microscopy inside the live worms without sophisticated sample preparation techniques and 3) there is a well-established and simple methodology to estimate the toxic effects of nanomaterials based on certain physiological parameters of microworms.

We investigated the toxicity of the pristine halloysite nanotubes (Figure 1 a) obtained from Applied Minerals Dragon Mine, USA which is also one of the products distributed by Aldrich-Sigma referred in many halloysite publications. Scanning electron microscopy image (Figure 1 b) confirms the typical sizes of the halloysite nanotubes (ca. 15 nm lumen and 50 nm outer diameter, and 1-1.5  $\mu\text{m}$  length). Importantly, halloysite nanotubes suspended in aqueous solutions can be visualised *in situ* using enhanced dark-field (EDF) microscopy. As shown in Figure 1 c, HNTs are clearly seen on the EDF microscopy image as bright spots retaining the intrinsic rod-like geometry (a real-time footage showing the movement of an isolated nanotube is shown in Video 1, in ESI). In water, HNTs exhibit the negative zeta-potential of  $-32 \pm 2$  mV.

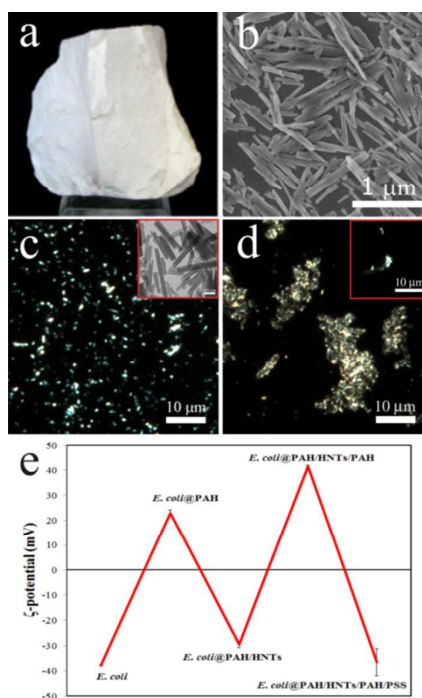


**Figure 1.** a) – A photograph of bulk halloysite mineral (size  $\sim 5$  cm); b) - SEM image of processed halloysite nanotubes. c) – HDRF microscopy image of HNTs dispersion in water, note the characteristic rod-like shape of the particles (inset shows a typical TEM image of the same sample); d) - HDRF microscopy image of polyelectrolytes-HNTs-coated *E. coli* cells (inset shows a partially coated cell demonstrating the direct attachment of nanotubes to the cell wall); e) – zeta-potential of *E. coli* cells as a function of deposited coating

The primary pathway of nanoparticles entry into nematodes is the intestinal uptake,<sup>32</sup> occurring while the worms feed on *E. coli* bacteria and spontaneously ingest the nanoparticles. However, HNTs' linear dimensions are large enough to anticipate that the worms may try avoiding the areas enriched with the nanotubes. Accordingly, we applied a simple behavioural test to assess the taxis of *C. elegans* microworms towards the HNTs. Starved L1 nematodes were introduced into the agar-based nematode growth media (NGM) on Petri dishes where 50  $\mu\text{L}$  of pure food (*E. coli*,  $10^{10}$  cells  $\text{mL}^{-1}$ ) and bacteria directly mixed with HNTs ( $1 \text{ mg mL}^{-1}$ ) were dropped onto the opposite sides of the dish, as demonstrated in Figure S1 in ESI. After 8 hours, the dishes were screened under a stereomicroscope to count the number of worms feeding on pure and HNTs-

mixed bacteria. Most of the worms (63%) were detected feeding on pure *E. coli*, while just the remaining 37% were spotted in HNTs-doped spots. Noteworthy, the animals found on HNTs-containing bacteria drops were considerably smaller than the ones found on HNTs-free drops (Figure S2 in ESI). This suggests that the worms actively avoid HNTs mixed with food, preferring the pure bacteria ration. We hypothesized that testing the toxic effects of HNTs using the traditional approach based on mixing bacterial food with nanoparticles<sup>37</sup> can be influenced by the behaviour of the worms trying deliberately to choose the HNTs-free bacterial cells during feeding. To overcome this, we employed the recently proposed nanoparticle delivery method based on “nanobaits” – microbial cells coated with nanoparticles sandwiched between polyelectrolyte nanolayers.<sup>38</sup> We deposited halloysite nanotubes on *E. coli* cells via the sequential layer-by-layer deposition of (poly)allylamine (PAH) and (poly)styrene sulphonate (PSS) polymers. The final architecture of nanocoatings on bacteria was: PAH/HNTs/PAH/PSS, to ensure the resulting negative charge of HNTs-coated cells, similar to that of intact cells. The effective immobilisation of HNTs on *E. coli* cells was confirmed by EDF microscopy (Figure 1 d) and by monitoring of zeta-potential inversion after each deposition step (Figure 1 e). Next, the HNTs-coated *E. coli* “nanobaits” were supplied to the *C. elegans* nematodes as the sole food source. Synchronised adult hermaphrodite animals were starved overnight, then the HNTs-coated cells were added onto the Petri dishes and the worms were allowed to feed freely on them for 1 hour. Next, the animals were collected and fixed for microscopy monitoring of HNTs localisation.

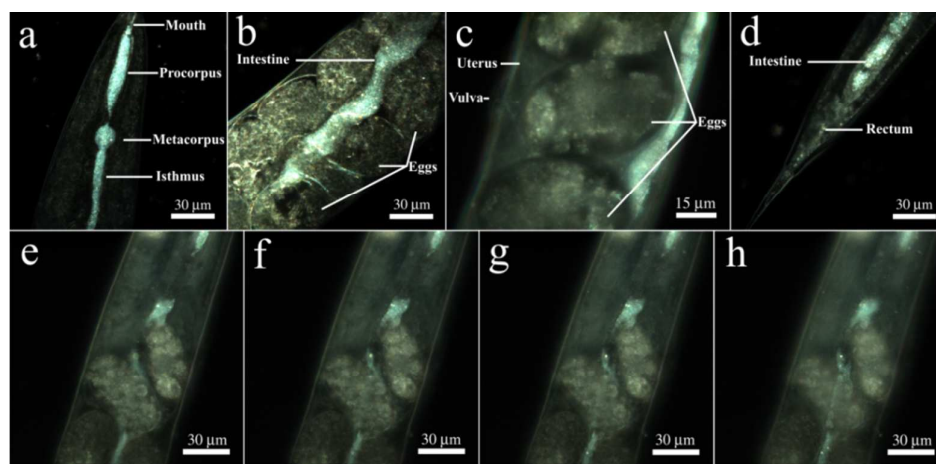


**Figure 2.** EDF microscopy images demonstrating the localisation of HNTs in nematodes’ intestines: a) – inside the foregut; b) and c) – in the midgut (note the absence of HNTs in embryos, uterus and vulva); d) – inside the hindgut; e-h) – EDF images of the intestine near the uterus taken at different focal planes demonstrate the localisation of HNT exclusively inside the intestine.

First, we labelled HNTs with rhodamine B prior to exposure to nematodes, and then inspected the sample with confocal microscopy, to find out that the confocal images do not allow us to visualise the HNTs inside the worms with the same precision as EDF microscopy (Figure S3 in ESI). High contrast of dark-field images of HNTs ingested during the feeding of the worms on HNTs allowed for the effective visualisation of the nanotubes without use of fluorescent dyes,<sup>32</sup> which may leak from the carrier particles or chemical fixation and thin-sectioning followed by electron microscopy imaging, which may result in washing off the nanotubes from the worms. On EDF microscopy images, halloysite nanotubes were found exclusively in the alimentary system of the worms (Figure 2 a-d). We detected the HNTs along the whole intestine, starting from buccal cavity to the anus, with prominent aggregations in interior bulb and terminal bulb (Figure 2 a). In the midgut and hindgut areas, HNTs were also clearly visible, however, less

aggregation was observed (Figure 2 b,d). The distribution of HNTs in a whole nematode is shown in Video 2 (ESI). Importantly, we did not detect nanotubes outside the intestines of the nematodes. Previous reports suggest that silica nanoparticles entry into *C. elegans* occurs not only through the mouth, but also through the vulva, whence they travel further and are consequently internalised by single vulval cells.<sup>37</sup> In case of HNTs, we do not see any aggregation of nanotubes near vulva (Figure 2 c), moreover, no free HNTs were detected inside the uterus or in embryos, suggesting that no uptake happens through vulva. We attribute this to the relatively large sizes of HNTs (up to 1500 nm), if compared with 50-nm silica used in the previous study.<sup>37</sup> Importantly, no HNTs were detected in vulva, ovaries or spermatheca in samples where the worms were incubated with free HNTs (data not shown), suggesting that HNTs not immobilised onto *E. coli* cells do not enter the vulva as well. More clearly the intestinal localisation of HNTs in nematodes can be seen in Figure 2 e-h. In this image, the focal plane was moved to demonstrate the intestine filled with randomly distributed HNTs, whereas no nanotubes were detected outside the intestines at the same focal planes. Interestingly, no HNTs were detected in embryos, which corresponds well with the inhomogeneous distribution of oxidised single-walled carbon nanotubes in *C. elegans*.<sup>32</sup>

Next, we investigated the toxic effects of HNTs by monitoring several physiological parameters of HNTs-treated nematodes. First, we focused on the body size of the worms (Figure 3 a), which is one of the integral parameters of toxic effects. HNTs within 0.05-1 mg mL<sup>-1</sup> concentration range inhibited the normal body growth of the nematodes if compared with the untreated samples, indicating the development deficit. However, the ingestion of HNTs-coated *E. coli* cells does not reduce the body size as much as reported for amine-modified single-walled carbon nanotubes,<sup>39</sup> where almost a two-fold reduction of the body length in *C. elegans* was detected. This suggests that the uptake of HNTs with food does not induce the starvation of the animals, more likely a different mechanism is responsible for the size reduction.

As noted, the reproductive organs, such as ovaries, uterus and spermatheca were free of HNTs. To explore the possible effects of HNTs onto the reproduction of the worms, the number of the eggs per hermaphrodite in HNTs-treated worms was counted (Figure 3 b). As expected, we found that HNTs have no significant effect on fertility of the microworms, no statistically significant reduction of egg number occurred.

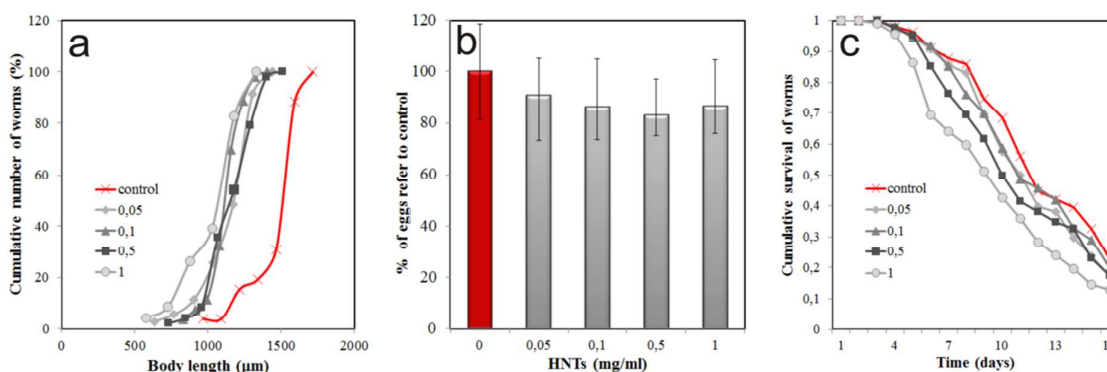


**Figure 3.** *In vivo* effects of HNTs on *C. elegans* growth and fertility: a) the cumulative curves of body length of nematodes treated with increasing concentrations of HNTs (mg mL<sup>-1</sup>) (n >100); b) – the influence of increasing concentration of HNTs on fertility in adult hermaphrodites (n >100); c) – cumulative nematode survival curve for increasing concentrations of HNTs (mg mL<sup>-1</sup>).

Finally, we investigated the longevity of the HNTs-treated *C. elegans*. Synchronised adult nematodes were kept in 96-well plates (~10 worms per well), treated with fluorodeoxyuridine (to inhibit the reproduction), then fed with HNTs-coated bacteria ( $100 \mu\text{L}^{-1}$ ) and monitored for viability by touching with a thin wire (the non-viable worms were counted if no tactile reaction was detected). Cumulative survival analysis demonstrated that no significant negative effect on the lifespan was induced in nematodes within all the concentrations of HNTs studied (Figure 3 c). The detailed statistical analysis of data presented in Figure 3 c is shown in Table S1 (ESI). Lower concentrations of HNTs ( $0.05, 0.1 \text{ mg mL}^{-1}$ ) did not decrease the longevity of the worms, whereas the higher concentrations ( $0.5, 1 \text{ mg mL}^{-1}$ ) somewhat reduced the mean lifespan (up to ~15% if compared with untreated animals), although this reduction was not statistically significant ( $P > 0.05$ ).

The results obtained suggest that HNTs have no profound toxic effects on *C. elegans* nematodes unlike other nanomaterials, such as single-walled<sup>39</sup> or multi-walled<sup>31</sup> carbon nanotubes, graphene oxide,<sup>40</sup>  $\text{TiO}_2$  nanoparticles<sup>40</sup> or platinum nanoparticles.<sup>41</sup> We suppose that the low toxicity of HNTs in comparison with other nanomaterials is outlined by the relatively low (if any) uptake of nanotubes by intestinal cells and very limited transport to other tissues and organs. For instance, highly-soluble single-walled carbon nanotubes (SWCNTs) severely reduced the body length in nematodes, whereas pristine SWNTs were almost not toxic.<sup>39</sup> Here, HNTs are ingested by nematodes via feeding on HNTs-coated cells, but then they are not adsorbed by the intestinal cells due to their sizes and are later safely removed via excretion. This is confirmed by observing the nematodes 2 hours after feeding (Figure S4 in ESI). Additionally, we performed another set of experiments, where we coated *C. elegans* eggs with PAH\HNTs\PAH\PSS (Figure 4 inset) and then incubated them normally and monitored HNTs in larvae and adult worms. In all cases, we did not detect any HNTs inside the animals. Moreover, only a slight reduction in body length was observed in nematodes hatched from HNTs-coated eggs (Figure 4). In this case, the microworms can take up the nanotubes through the egg cuticle only, and after hatching the nematodes apparently try to avoid ingesting nanotubes during feeding on bacteria.

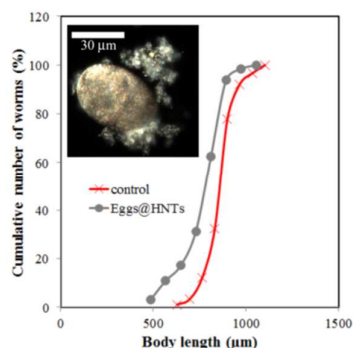


**Figure 4.** The cumulative curves of body length of nematodes hatched from the HNTs-coated eggs (inset shows a typical EDF microscopy image of HNTs-coated egg)

Finally, we tried to elucidate the mechanism of the slight toxic effect of higher concentrations of HNTs on body length of the nematodes. We suppose that this might be caused by the irritation inflicted by rod-shaped nanotubes contacting with the intestinal cuticle of the worms. Using the EDF microscopy, we observed the spontaneous intensive rotational movement of single isolated nanotubes and larger aggregates of nanotubes inside the intestines of the immobilised living adult nematodes along the whole length of the gut. Typical real-time footages demonstrating these movements in grinder and intestines are given in ESI (Video 3 and Video 4, respectively). We suppose that the moving nanotubes can harm and irritate the intestines of microworms, thus affecting the ingestion, and, as a consequence, the body length, whereas the number of the eggs

and the overall longevity is not reduced. Normally, micron-sized food particles (bacterial cells) as well as artificial microparticles reside in the intestine for around 60-110 seconds, being constantly excreted from the hindgut during defecation.<sup>42</sup> The very fast digestion and excretion of bacteria provides the nematodes with nutrients, however, in our study, we found that HNTs persisted in intestines even after 2 hours upon ingestion (after feeding with HNTs-coated bacteria, the worms were transferred into HNTs-free dishes). The EDF microscopy images of the nematodes (data not shown) clearly demonstrate that the nanotubes are still seen inside the intestines, although in this case they are primarily located in the hindgut region, which suggests that HNTs migrate very slowly if compared with normal diet (*E. coli*) or 2  $\mu\text{m}$  polystyrene beads.<sup>42</sup> It is likely that the HNTs reversibly adsorb onto intestinal microvilli and thus irritate the intestinal cells. Noteworthy, no bacterial layers were observed inside the intestine,<sup>44</sup> suggesting that the irritating HNTs effect is temporary, and worms eventually restore the normal digestion. However, the persisting aggregates and moving nanotubes are expected to induce the acute effects onto digestion, which is supported by the reduced body sizes of HNTs-treated nematodes.

### **Conclusions**

Our study suggests that the HNTs within the concentrations investigated are not capable to severely damage the organism of the nematodes, inflicting only mechanical stress onto the alimentary system. We believe that the microworms intentionally avoid the nanotubes, therefore the only effective way of delivery is based on HNTs-modified cells. Regarding the potential applications of HNTs in *C. elegans* studies, pH-sensitive sensors, currently fabricated using silica nanoparticles,<sup>43</sup> in future can be produced using HNTs, considerably reducing the unwanted toxic effects of silica.<sup>37</sup> During manufacturing and halloysite product usage, these aluminosilicate nanotubes will be eventually returned to the environment as fine nano-powder, therefore its toxicity assessment is important. Overall, low toxicity of halloysite to soil nematodes demonstrated in this work suggests that its quickly growing industrial application are likely to be environmentally safe.

### **Acknowledgement**

The work is performed according to the Russian Government Program of Competitive Growth of Kazan Federal University. This work was funded by the subsidy allocated to Kazan Federal University for the state assignment in the sphere of scientific activities. This publication is based on work supported by a grant FSAX-14-60155-0 from the U.S. Civilian Research & Development Foundation (CRDF Global). Any opinions, findings and conclusions or recommendations expressed in this material are those of the authors and do not necessarily reflect the views of CRDF Global.

**Electronic supporting information** is available: experimental details, additional Figures, a Table and real time footages, as noted in the text.

### **References**

1. Y. Lvov and E. Abdullayev, *Prog. Polym. Sci.*, 2013, **38**, 1690-1719.
2. E. Abdullayev, A. Joshi, W. Wei, Y. Zhao and Y. Lvov, *ACS Nano*, 2012, **6**, 7216-7226.
3. N. Veerabadran, R. Price and Y. Lvov, *NANO Journal*, 2007, **2**, 215-222.
4. V. Vergaro, Y. Lvov and S. Leporatti, *Macromol. Bioscience*, 2012, **12**, 1265-1271.
5. Y. Lee, G. Jung, S.J. Cho, K.E. Geckeler and H. Fuchs, *Nanoscale*, 2013, **5**, 8577-8585.
6. K. M. Rao, S. Nagappan, D. J. Seo and C.-S. Ha, *Applied Clay Science*, 2014, **97-98**, 33-42.

7. C. Chao, J. Liu, J. Wang, Y. Zhang, B. Zhang, Y. Zhang, X. Xiang and R. Chen, *ACS Appl. Mater. Interfaces*, 2013, **5**, 10559–10564.
8. Y. Shi, Z. Tian, Y. Zhang, H. Shen and N. Jia, *Nanoscale Res. Lett.*, 2011, **6**:608. DOI: 10.1186/1556-276X-6-608.
9. W. Wei, R. Minullina, E. Abdullayev, R. Fakhrullin, D. Mills and Y. Lvov, *RSC Advances*, 2014, **4**, 488-494.
10. A.D. Hughes and M. R. King, *Langmuir*, 2010, **26**, 12155–12164.
11. M.J. Mitchell, C.S. Chen, V. Ponmud, A.D. Hughes and M.R. King, *J. Control. Release*, 2012, **160**, 609-617.
12. S.A. Konnova, I.R. Sharipova, T.A. Demina, Y.N. Osin, D.R. Yarullina, O.N. Ilinskaya, Y.M. Lvov and R.F. Fakhrullin, *Chem. Commun.*, 2013, **49**, 4208-4210.
13. M. Liu, C. Wu, Y. Jiao, S. Xiong and C. Zhou, *J. Mater. Chem. B*, 2013, **1**, 2078–2089.
14. G. Cavallaro, G. Lazzara, S. Milioto, F. Parisi and V. Sanzillo, *ACS Appl. Mater. Interfaces*, 2014, **6**, 606-612.
15. E. Abdullayev, V. Abbasov, A. Tursunbayeva, V. Portnov, H. Ibrahimov, G. Mukhtarova and Y. Lvov, *ACS Appl. Mater. Interfaces*, 2013, **5**, 4464–4471.
16. E. Abdullayev, R. Price, D. Shchukin and Y. Lvov, *ACS Appl. Mater. Interfaces*, 2009, **1**, 1437–1443.
17. J. Qiao, J. Adams and D. Johannsmann, *Langmuir*, 2012, **28**, 8674–8680.
18. J. Zhang, Y. Zhang, Y. Chen, L. Du, B. Zhang, H. Zhang, J. Liu, and K. Wang, *Ind. Eng. Chem. Res.*, 2012, **51**, 3081–3090.
19. L. Wang, J. Chen, L. Ge, Z. Zhu and V. Rudolph, *Energy Fuels*, 2011, **25**, 3408–3416.
20. L. Wang, J. Chen, L. Ge, V. Rudolph and Z. Zhu, *J. Phys. Chem. C*, 2013, **117**, 4141–4151.
21. Y. Fu, D. Zhao, W. Wang and Y. Lvov, *IOP Mater. Sci. Eng. J.*, 2014, **53**, 132-136.
22. M. Du, B. Guo and D. Jia, *Polymer Intern.*, 2010, **59**, 574-595.
23. V. Vergaro, E. Abdullayev, Y. M. Lvov, A. Zeitoun, R. Cingolani, R. Rinaldi and S. Leporatti, *Biomacromolecules*, 2010, **11**, 820–826.
24. X. Lai, M. Agarwal, Y. Lvov, C. Pachpande, K. Varahramyan and F. Witzmann, *J. Appl. Toxicity*, 2013, **33**, 1316-1329.
25. M.C. Bottino, G.H. Yassen, J.A. Platt, N. Labban, L.J. Windsor, K.J. Spolnik and A.H. Bressiani, *J Tissue Eng Regen Med.*, 2013, DOI: 10.1002/term.1712.
26. Y. Zhang, Y. Chen, H. Zhang, B. Zhang and J. Liu, *J. Inorg. Biochem.*, 2013, **118**, 59–64.
27. H.-J. Choi, T.J. Stazak Jr. and C. D. Montemagno, *J. Nanopart. Res.*, 2013, **15**:2008. DOI: 10.1007/s11051-013-2008-4.
28. J. S. Bozich, S. E. Lohse, M. D. Torelli, C. J. Murphy, R. J. Hamers and R. D. Klaper, *Environ. Sci.: Nano*, 2014, **1**, 260-270.
29. E. Culetto and D. B. Sattelle, *Hum. Mol. Genet.*, 2000, **9**, 869-877.
30. T. Kaletta and M. O. Hengartner, *Nat. Rev. Drug. Discov.*, 2006, **5**, 387-399.
31. A. Nouara, Q. Wu, Y. Li, M. Tang, H. Wang, Y. Zhao and D. Wang, *Nanoscale*, 2013, **5**, 6088-6096.
32. C. M. Goodwin, G. G. Lewis, A. Fiorella, M. D. Ellison and R. Kohn, *RSC Adv.*, 2014, **4**, 5893-5900.
33. S. W. Kim, J. I. Kwak and Y.-J. An, *Environ. Sci. Technol.*, 2013, **47**, 5393-5399.
34. A. Pluskota, E. Horzowski, O. Bossinger and A. von Mikecz, *PLoS one*, 2009, **4**, e6622.
35. W. Zhang, B. Sun, L. Zhang, B. Zhao, G. Nie and Y. Zhao, *Nanoscale*, 2011, **3**, 2636-2641.
36. E. Zanni, G. De Bellis, M. P. Bracciale, A. Broggi, M. L. Santarelli, M. S. Sarto, C. Palleschi and D. Uccelletti, *Nano Letters*, 2012, **12**, 2740-2744.
37. A. Scharf, A. Piechulek, and A. von Mikecz, *ACS Nano*, 2013, **7**, 10695–10703
38. G.I. Däwläšina, R.T. Minullina and R.F. Fakhrullin, *Nanoscale*, 2013, **5**, 11761-11769.
39. P.-H. Chen, K.-M. Hsiao and C.-C. Chou, *Biomaterials*, 2013, **34**, 5661-5669.

40. Q. Wu, Y. Zhao, G. Zhao and D. Wang, *Nanomedicine*, 2014, **10**, 1263-1271.
41. J. Kim, T. Shirasawa and Y. Miyamoto, *Biomaterials.*, 2010, **31**, 5849-5854.
42. S. Ghafouri and J.D. McGhee, *Nematology*, 2007, **9**, 87-91.
43. N.D. Mathew, M.D. Mathew and P.P. Surawski, *Anal. Biochem.*, 2014, **450**, 52-56.
44. Y. J. Cha, J. Lee and S.S. Choi, *Chemosphere*, 2012, **87**, 49-54.